Geochimica et Cosmochimica Acta, Vol. 69, No. 8, pp. 2095–2109, 2005

0016-7037/05 $30.00 + .00

doi:10.1016/j.gca.2004.10.024

Trace element cycling in a subterranean estuary: Part 1. Geochemistry of the permeable sediments

Matthew A. Charette,[1,*] Edward R. Sholkovitz,[1] and Colleen M. Hansel[2,†]

[1]Department of Marine Chemistry and Geochemistry, Woods Hole Oceanographic Institution, Woods Hole, MA 02543, USA
[2]Department of Geological and Environmental Sciences, Stanford University, Stanford, CA 94305, USA

(*Received February* 17, 2004; *accepted in revised form October* 25, 2004)

Abstract—Subterranean estuaries are characterized by the mixing of terrestrially derived groundwater and seawater in a coastal aquifer. Subterranean estuaries, like their river water-seawater counterparts on the surface of the earth, represent a major, but less visible, hydrological and geochemical interface between the continents and the ocean. This article is the first in a two-part series on the biogeochemistry of the subterranean estuary at the head of Waquoit Bay (Cape Cod, MA, USA). The pore-water distributions of salinity, Fe and Mn establish the salt and redox framework of this subterranean estuary. The biogeochemistry of Fe, Mn, P, Ba, U and Th will be addressed from the perspective of the sediment composition. A second article will focus on the groundwater and pore-water chemistries of Fe, Mn, U and Ba.

Three sediment cores were collected from the head of Waquoit Bay where the coastal aquifer consists of permeable sandy sediment. A selective dissolution method was used to measure the concentrations of P, Ba, U and Th that are associated with "amorphous (hydr)oxides of iron and manganese" and "crystalline Fe and Mn (hydr)oxides." The deeper sections of the cores are characterized by large amounts of iron (hydr)oxides that are precipitated onto organic C-poor quartz sand from high-salinity pore waters rich in dissolved ferrous iron. Unlike Fe (hydr)oxides, which increase with depth, the Mn (hydr)oxides display midcore maxima. This type of vertical stratification is consistent with redox-controlled diagenesis in which Mn (hydr)oxides are formed at shallower depths than iron (hydr)oxides. P and Th are enriched in the deep sections of the cores, consistent with their well-documented affinity for Fe (hydr)oxides. In contrast, the downcore distribution of Ba, especially in core 3, more closely tracks the concentration of Mn (hydr)oxides. Even though Mn (hydr)oxides are 200–300 times less abundant than Fe (hydr)oxides in the cores, Mn (hydr)oxides are known to have an affinity for Ba which is many orders of magnitude greater than iron (hydr)oxides. Hence, the downcore distribution of Ba in Fe (hydr)oxide rich sediments is most probably controlled by the presence of Mn (hydr)oxides. U is enriched in the upper zones of the cores, consistent with the formation of highly reducing near-surface sediments in the intertidal zone at the head of the Bay. Hence, the recirculation of seawater through this type of subterranean estuary, coupled with the abiotic and/or biotic reduction of soluble U(VI) to insoluble U(IV), leads to the sediments acting as a oceanic net sink of U. These results highlight the importance of permeable sediments as hosts to a wide range of biogeochemical reactions, which may be impacting geochemical budgets on scales ranging from coastal aquifers to the continental shelf.

1. INTRODUCTION

Geochemical studies of coastal marine sediments have typically focused on fine-grained cohesive deposits. High concentrations of organic matter and clay minerals in these muddy and silty sediments lead to chemical and mineral diagenesis involving the microbial degradation of organic matter and the development of redox gradients (Froelich et al., 1979; Aller, 1980). Permeable sediments, which constitute a large fraction of sediments in coastal aquifers, intertidal zones and continental shelves throughout the world, consist primarily of coarse-grained sands low in organic matter. By their nature, permeable sediments are more open to the advective transport of water, dissolved solutes and fine suspended particles, which results from the action of groundwater transport, waves and tides. Permeable sediments typically undergo suboxic rather than anoxic chemical diagenesis as observed in many cohesive sediment deposits (Slomp et al., 1997; Kristensen et al., 2002, 2003).

Despite the relatively low solute concentrations found in permeable sediments, the solute fluxes to the overlying water column may be large because flow rates may be orders of magnitude greater than from fine-grained sediments. This results in relatively high solute fluxes to the overlying water column (Huettel and Gust, 1992; Huettel et al., 1996, 1998; Huettel and Rusch, 2000; Rusch and Huettel, 2000; Roy et al., 2002; Jahnke et al., 2003; Precht and Huettel, 2003). The field studies and flume experiments of Huettel et al. (1998) revealed that permeable sediments from the North Sea undergo a variety of diagenetic reactions that include the consumption of dissolved oxygen and organic matter and the production of metabolic nutrients. Reimers et al. (2004) demonstrated a positive correlation between flow and oxygen consumption in permeable sediments of the USA Middle Atlantic Bight.

* Author to whom correspondence should be addressed (mcharette@whoi.edu).
† *Present address:* Department of Biology, Woods Hole Oceanographic Institution, Woods Hole, MA 02543, USA.

The permeable sediments that characterize sandy beaches, which are often influenced by groundwater flowing through coastal aquifers toward the sea, have also been overlooked as zones of biogeochemical transformations. This led Moore (1999) to introduce the concept of a "subterranean estuary," which he defined as the mixing zone between terrestrially derived fresh groundwater and seawater in a coastal aquifer. Subterranean estuaries, like their river water-seawater counterparts on the surface of the earth, represent a major, but less visible, hydrological interface between the continents and the ocean. With respect to "surface estuaries," the river transport of solutes, colloids and suspended particles and reactions during the mixing of river water and seawater play a major role in the biogeochemical cycles of many inorganic elements in the oceans (e.g., Boyle et al., 1977; Li and Chan, 1979; Edmond et al., 1985; Coffrey et al., 1997). In contrast to the large literature on the hydrology, estuarine chemistry and biogeochemistry of surface estuaries, subterranean estuaries have not been studied in any systematic fashion (Moore and Shaw, 1998; Burnett et al., 2001, 2002). However, recent studies indicate that the oceanic budgets of alkaline earth elements (Ba, Sr and Ra) must be reevaluated from the perspective of submarine groundwater discharge and biogeochemical reactions within subterranean estuaries (Moore, 1996; Shaw et al., 1998; Basu et al., 2001).

This article is the first of a two-part series on the biogeochemistry of the Waquoit Bay coastal aquifer/subterranean estuary. This first article will use the pore-water distributions of salinity, Fe and Mn to establish the salinity and redox framework of the subterranean estuary. It will then address the biogeochemistry of Fe, Mn, P, Ba, U, and Th from the perspective of the sediments. By focusing on this group of elements, four important classes of reactions (and reactants) are studied. These include [1] redox-controlled solubility (Fe, Mn and U), [2] adsorption (P, Th, Ba, Ra) onto the oxides of Fe and Mn, [3] release (P, Ba, Ra) from oxides undergoing reductive dissolution, and [4] desorption (Ba, Ra) from sediments via ion-exchange reactions.

The second article will use groundwater, pore-water and Bay surface water data to establish a more detailed view into the estuarine chemistry and the chemical diagenesis of Fe, Mn, U and Ba in the coastal aquifer. By focusing on a small and well-defined subterranean estuary (Waquoit Bay, MA, USA), these two articles will provide an in-depth study of the major biogeochemical reactions operating on the permeable sediments of a coastal aquifer with active Fe and Mn redox cycles and well-defined salinity gradients.

2. STUDY AREA

Waquoit Bay is a shallow semi-enclosed estuary located on the south shoreline of Cape Cod (MA, USA; Fig. 1). The bay is tidally flushed with Vineyard Sound through a narrow inlet to the south. The sedimentary deposits of the study area generally consist of outwash gravel, sand and silt with occasional lacustrine deposits of silts and clays (Oldale, 1976). Several characteristics make this bay an ideal natural laboratory to study the biogeochemistry of subterranean estuaries and their impact on the coastal ocean.

First, because the soil on Cape Cod is primarily composed of coarse-grained sand, precipitation tends to infiltrate the sediments rather than become surface runoff. Thus, groundwater is the major source of freshwater to the bay and to the two rivers that drain into it (Cambareri and Eichner, 1998; Valiela et al., 1990; Charette et al., 2001; U.S. Geological Survey, 2003). Second, along the shoreline of Waquoit Bay, the upper ~10 m of the Cape Cod aquifer consists of a relatively homogeneous distribution of highly permeable sediment (Cambareri and Eichner, 1998) which results in a well-confined subterranean estuary (Testa et al., 2002; Talbot et al., 2003). This sediment forms the end moraine deposit from the late Wisconsinan deglaciation of ~12,000 to 15,000 yr ago (Oldale, 1981).

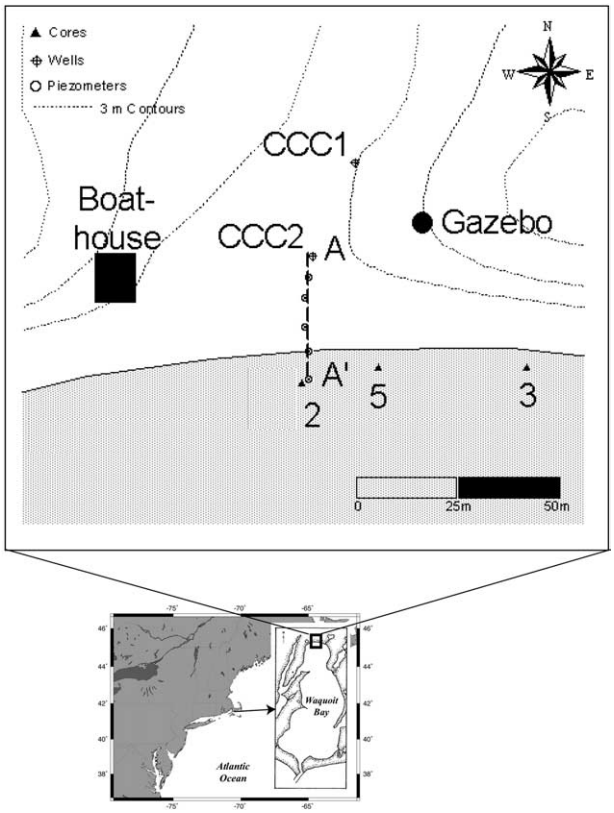

Fig. 1. Location within Waquoit Bay of the vibracores discussed in this article. Also included is the location of the July 2002 piezometer transect (A to A′) used to collect pore-water profiles and the locations of the two multilevel monitoring wells (CCC1 and CCC2).

Waquoit Bay, due to its status as a National Estuarine Research Reserve, has been the focus of many prior studies documenting the importance of submarine groundwater discharge (SGD) on nutrient budgets and water balances (e.g., Valiela et al., 1990; Charette et al., 2001; Abraham et al., 2003; Michael et al., 2003). For example, seepage meter studies indicate that submarine groundwater discharge occurs in a narrow (~25 m wide) band along the head of the bay (Michael et al., 2003; Sholkovitz et al., 2003). Surface water samples collected by Charette et al. (2001) show that the head of the Bay is less saline and have higher activities of Ra isotopes than the ocean end of Bay. Their Ra isotope based estimate of SGD confirms that the input of fresh and brackish groundwater is an important process at the head of the Bay.

3. EXPERIMENTAL METHODS AND PROCEDURES

3.1. Field Methods

A series of sediment cores and pore-water (groundwater) samples were obtained from the beach at the head of Waquoit Bay during 2001 and 2002 (Fig. 1). This region of the bay is well protected from waves and storms that would otherwise rework the sands. Five sediment cores, ranging from 1.1 to 2.0 m in length, were collected in 1 d in April 2001 using a vibracoring technique. Photographs of the vibracoring unit and the sediment from core 1 can be found on the May 15, 2002, cover of *Geophysical Research Letters* (Volume 29, No 10). Color photographs of cores 2, 3 and 5 can be found in Charette and Sholkovitz (2002). Only cores 2, 3 and 5 will be discussed in this article. After collecting the cores, the aluminum core barrels (7.6 cm diameter) were returned to laboratory that afternoon and split length-wise; the cores were then sectioned into 5-cm increments. The recovered lengths of cores 2, 3 and 5 were 175, 112, and 169 units of cm respectively. We observed a shortening of the cores relative to the penetration of their core barrels into the sediments. Sediment compaction by the vibracoring technique is a likely explanation. Compression factors were 1.5, 1.7 and 1.5 for cores 2, 3 and 5 respectively. The depth scales used in this article were not corrected for compaction. The pore water within the permeable sands of these cores drained away during the extrusion and sectioning activities. Hence, the solid phase data for these cores are not accompanied by pore-water data.

Charette and Sholkovitz (2002) reported the Fe and P concentrations of cores 2, 3, and 5. These cores were selected for more comprehensive chemical analyses because they each had a unique color stratigraphy resulting from the dominance of various forms of iron (hydr)oxides. We also analyzed two types of "control" sediment: (1) surface beach sand from the head of Waquoit Bay near the coring sites, and (2) offsite sand collected from a Vineyard Sound beach (Surf Drive Beach) located 10 km from Waquoit Bay. The former sediment will be referred to as sample WB and the latter as sample PB. The offsite location was chosen as it contains local quartz-rich sand that is visibly clean and free of oxide coatings.

Piezometers were used to obtain a two dimensional distribution of the pore-water composition at the head of Waquoit in 2002. As shown in Figure 1, six piezometer profiles were sited along a 17 m transect (A–A′) that extends from the berm of the beach to the low tide watermark. Each profile required 4 to 8 h of sampling, and the complete transect covered 17 d (7 June to 3 July). Hence, the pore-water data do not represent synchronous distributions of the measured parameters.

Depth profiles of pore-water samples were obtained with a stainless steel drive point piezometer system ("Retract-A-Tip" from AMS Inc.). Briefly, the sampling port near the tip of the piezometer was hand driven into the beach sediment. Pore-water samples were brought to the surface through acid-cleaned Teflon or polypropylene tubing using a peristaltic pump. This system allowed us to collect profiles to a depth of 8 m with a sampling interval as small as 0.2 m. After flushing the tubing several times, samples were directly filtered into acid cleaned LDPE bottles using an all-plastic syringe and an in-line 0.2-μm capsule filter. The samples were immediately acidified to pH 1 with trace metal grade HCl. Salinity was measured in the field using a YSI 600R multiprobe in a flow through cell (YSI, Inc.).

3.2. Laboratory Methods and Analysis

Core sediments and beach sands were air dried and hand-sieved through a polypropylene mesh with a nominal retention diameter of 1 mm. Sieved sediment was used in all subsequent measurements. The major fraction of the sediments passed through the 1 mm sieve, though the near-surface zone of some cores had centimeter-sized stones. Before organic carbon analysis, sediment samples were transferred to small vials and fumed with HCl in a desiccator to remove any carbonate minerals. The samples were then dried at 50°C for 48 h. Approximately 35 mg of sample was then weighed out in 5 × 8 mm ultra-clean tin capsules, and the samples were then analyzed for carbon on a CE Instruments Flash 1112 Series EA CHN analyzer.

The speciation and structural environment of Fe were determined using X-ray absorption spectroscopy (XAS) as described in detail previously (Hansel et al., 2003). A set of reference standards for Fe (for more details see Hansel et al., 2003), was utilized to perform linear combination k^3-weighted extended X-ray absorption fine structure (LC-EXAFS) spectral fitting using the EXAFSPAK module DATFIT (George, 1993). Linear fitting routines were used to reconstruct the unknown to determine the relative percentages of mineral phases within the samples. Linear combinations of empiric model spectra were optimized where the only adjustable parameters were the fractions of each model compound contributing to the fit. Fits were optimized by minimizing the residual, defined as the normalized root square difference between the data and the fit. Qualitative and quantitative confirmation of linear combination Fe EXAFS fits was investigated using Mössbauer spectroscopy and also fitting a set of mixed standards having known fractions (Hansel et al., 2003). Fits were within ±5% of the actual mole percentages using the k-range 1–14 $Å^{-1}$. The detection limit for minor constituents was ca. 5%.

The concentrations of iron and manganese (hydr)oxides in the sediments, along with their associated P, Ba, U and Th concentrations, were determined using the selective dissolution protocol of Hall et al. (1996). We used their L3 solution to dissolve "amorphous oxides of iron and manganese," followed by their L4 solution that targets "crystalline Fe and Mn (hydr)oxides." The sum of the L3 and L4 leaches is referred to a "total oxide" composition. With all selective dissolution schemes, specificity is difficult to quantify and the results are method dependent. This is particularly the case when dealing with the iron and manganese (hydr)oxides, which exist in many mineral forms and oxidation states. Hence, the transition from amorphous to crystalline forms of Fe is not a sharp one. With this provision in mind, certain trends in the L3 vs. L4 profiles provide a basis for better understanding the geochemistry of the Waquoit Bay cores.

The L3 and L4 leaches were performed in series on the same aliquot of sediment. Each leach was performed twice on ~0.4 g of sample and combined to yield one L3 and one L4 solution per sample for chemical analyses. The L3 leach solution consists of 10 mL of 0.25 M hydroxylamine hydrochloride in 0.05 M HCl; sample plus leach was heated for 2 h at 60°C. The sediment was allowed to settle to the bottom of the Teflon reaction vessel and the L3 solution was carefully pipetted into a small acid cleaned LDPE bottle. The L3 leaching step was repeated on the same aliquot of sediment. The L4 solution was then added to the sediment in the original reaction vessel. The L4 solution, which consists of 25 mL of 1 M hydroxylamine hydrochloride in 25% glacial acid, was heated at 90°C for 3 hrs. After allowing the to settle, the L4 solution was carefully pipetted into a small acid cleaned LDPE bottle. Finally, this L4 leaching step was repeated as outlined above.

The phosphorous concentration of the sediment leaches was determined by using the ammonium molybdate method on a Lachat QuickChem 8000 flow injection analyzer. Subsamples of the L3 and L4 leaches were diluted with clean water (1:6) before analysis.

Inductively couple plasma mass spectrometry (ICP-MS) was used to measure the concentrations of Fe, Mn, Ba, U and Th in the sediment leaches. Aliquots of the L3 and L4 solutions were diluted with Milli-Q water (1:20 to 1:100) before analysis. Standards were prepared in similarly diluted L3 and L4 solutions to achieve the same matrix composition. Indium (In) was used as an internal standard to quantitatively account for variations in the performance of the mass spectrometer during analysis. A known quantity of In was added to samples and standards. The resulting In count rate data were used to normalize the mass spectrometer count rate for Fe, Mn, U, Ba and Th. A Finnigan element high resolution ICP-MS, operated by the WHOI mass spectrometry facility, was used in low-resolution mode for In (115), U (238), Ba (137) and Th (232) and in the medium-resolution mode for Mn(55), Fe(56), and In (115).

The iron concentrations of cores 2, 3 and 5, reported in Charette and Sholkovitz (2002), used the same L3 and L4 solutions but a different analytical method, the ferrozine spectrometric technique of Stookey (1970). A reductant (hydroxylamine hydrochloride) was added to diluted aliquots of each L3 and L4 solution. Each solution was heated to 60°C for 1 h, buffer and a ferrozine solutions were added and the absorbances of the resulting solutions were measured at 562 nm. This procedure measures total reducible iron which is Fe(II) plus reducible Fe(III).

The pore-water concentrations of total dissolved Fe and Mn were measured using ICP-MS following a 1:20 dilution of each sample with MQ water. Dissolved ferrous iron (Fe [II]) and total dissolved Fe (Fe

[II] + Fe [III] were also measured by ferrozine colorimeteric method of (Stookey, 1970). Only the ICP-MS Fe pore-water data will be presented in this article. Of importance to this study is the fact that ferrous (Fe [II]) comprises a major fraction of the total pore-water Fe.

A selected number of sediment samples were analyzed in duplicate and, in a few cases, triplicate. The average value of the replicate analyses are reported here. Duplicate colorimetric analyses of P have standard deviations that range from 5 to 25%; duplicate analyses ICP-MS analyzes of Fe, Mn, U and Th have deviations that range from 3 to 10%. The latter range is much greater than counting errors associated with ICP-MS analyses (1%–5%). We attribute these relatively high standard deviations to the fact that our leaching method only used small sediment aliquots (0.4 g) of sediments which, in turn, were visibly heterogeneous with respect to the distribution of colored iron (hydr)oxides within the sandy matrix of the samples.

For analysis of total uranium, ~50–150 g (dry wt.) of sediment (<1 mm) was weighed into 8-oz. polystyrene jars and analyzed on a planar-style pure Ge detector (2000 mm^2). The samples had been stored for ~1 yr before analysis, therefore ^{238}U was quantified by is daughter product (^{234}Th) at 63.3 keV. The program GESPECOR, a Monte Carlo based software used for calibration of pure Ge detectors, was used to calibrate the detector for various geometries described above (Sima and Arnold, 2002). Selected sediment samples from cores 2, 3, and 5 were subjected to grain size analysis at the Sedimentation Laboratory at the Woods Hole Field Center of the Coastal and Marine Geology Program of the U.S. Geological Survey.

4. RESULTS

4.1. Distribution of Pore-Water Salinity, Fe, Mn and Sulfate

The salinity distribution in Figure 2 shows that there is a well-defined subterranean estuary beneath the head of the Bay. This subterranean estuary has a narrow seepage face where zero salinity groundwater flows upward to the surface of the beach. Sharp salinity gradients exist over short distances in both the vertical and horizontal directions. For example, salinity increases from 0 to 28 over 2.5 vertical meters in piezometer 3, which lies in the center of the beach. With respect to the horizontal scale, the pore-water salinity in the upper meter of beach sediments increased from 0 to 28 over a distance of less than 10 m. The large salinity gradients result in a strong pycnocline, which leads to vertical and horizontal density stratification within the subterranean estuary. The salinity distributions are similar to those of well stratified or salt-wedge type surface estuaries where large rivers discharge over landward intruding seawater.

The pore-water distributions of Fe and Mn show that the subterranean estuary in Waquoit Bay is the site of active Fe and Mn redox reactions. There are two distinct sources of the high observed concentrations of total dissolved Fe and Mn. One source resides in the upward rising plume of freshwater, and the second source lies in the salt-wedge zone of mid- to high-salinity pore water. The distribution of Fe and Mn within the freshwater region of the subterranean estuary provides strong evidence that there is a plume of Fe/Mn-rich groundwater moving toward the Bay. This plume is centered between a depth of 2 and 4 m and carries up to 175 μM of Fe and 15 μM of Mn. As the leading edge of this plume moves upward toward the beach, almost all of the Fe and Mn is removed over a horizontal distance of only a few meters between stations 6 and 3. The upper and lower sections of the plume also exhibit large-scale decreases of Fe and Mn over vertical distances of only 1–3 m. Our unpublished data from wells CCC1 and CCC2, on the upland side of the berm (Fig. 1), confirm that the freshwater plume of high Fe and Mn extends landward for at least 30 m.

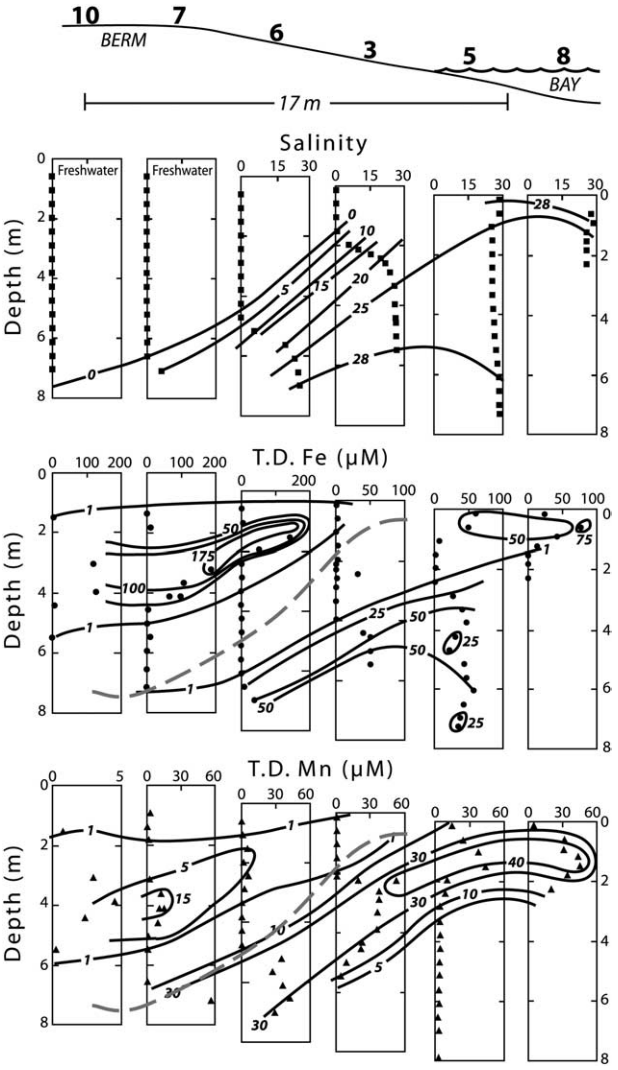

Fig. 2. Pore-water salinity and dissolved Fe and Mn contours in the subterranean estuary of Waquoit Bay. The data were collected from the A-A′ shore-perpendicular piezometer transect at the head of the Bay. The gray dashed line on the Fe and Mn contour plots indicates the location of the fresh-saline groundwater interface.

The second source of dissolved Fe and Mn lies in the salt wedge section of the subterranean estuary where pore-water concentrations reach 50 μM of Fe and 40 μM of Mn (Fig. 2). Piezometers 6 and 3, with their well-developed salt gradients, show that the high concentrations of Fe and Mn are associated with a salinity that exceeds 5–10. While maximum concentration of Fe in the freshwater plume exceeds that of the salt-wedge Fe by a factor of 3.5, Mn follows the opposite trend. Another key feature of the subterranean estuary is the fact that a lens of high Mn concentration lies over a lens of high Fe concentration. This is seen most clearly in the salt-wedge section of the estuary covered by piezometers 3 and 5 (Fig. 2).

Pore-water sulfate concentrations were only measured on

piezometer 3 samples, which cover the full salinity range of the subterranean estuary (Fig. 2). The sulfate concentrations range from 4.8 to 18.6 mmol/kg over the salinity range of 9.6 to 26.6. Relative to a sulfate to salinity ratios of 0.805 for open ocean seawater of 35 salinity, the high- (> 9.6) salinity pore waters have ratios of 0.5 to 0.7 which are equivalent to 57 to 88% of their seawater-derived sulfate content. This 12%–43% depletion of seawater-derived sulfate points to sulfate reduction. We did not focus on the sulfate-sulfide part of the Fe cycle as our cores showed no visual signs of iron sulfide and our pore-water samples lacked any smell of sulfide. However, we cannot conclusively rule out the precipitation of FeS or pyrite as a sink for iron in this system. While the production of sulfide from sulfate is occurring, these sediments are likely dominated by the formation of iron (hyrdr)oxides and by the redox cycles of Fe and Mn. There is one exception to this observation. The Bay has large algal blooms in the later spring and summer; this leads to the intertidal zone of the beach being covered with mats of organic matter. Areas of the beach which are ~ 200 m to the east of our coring sites have black iron sulfide coated sands in the summer. These sulfides can be found on the surface to a few centimeters below the surface. While less abundant near our sampling site, iron sulfides can be seen underlying a thin layer of oxic sand. The black iron sulfide is absent during the fall and winter.

The last feature of note in Figure 2 is the region of high Fe concentration that occurs in the high-salinity pore waters within the upper 50 cm of piezometers 5 and 8. This zone of high Fe lies in the seawater end of the subterranean estuary that coincides with intertidal region of the beach. We believe that the microbial decomposition of algae in this zone leads to reducing conditions and the formation of reduced Fe in the near-surface pore water.

4.2. Sedimentology and Type of Iron (Hydr)Oxide Precipitates

No systematic mineralogical study was carried out. The sediments (< 1 mm) in all cores consisted of coarse-grained sand. A microscope screening of core 2 sediment revealed that the majority of the monomineralic grains are quartz. There is <1% of plagioclase along with traces of clinopyroxene, amphibole, white mica, magnetite and at least one other oxide (goethite or hematite). Polymineralic fragments in the sands probably represent granite, schist, amphibolite and gabbro. Grain size analyses were carried out on surface sediments and on deeper sediments of cores 2, 3 and 5. The deeper sediments came from the iron (hydr)oxide rich horizons. All six samples (surface and deep) had similar size distributions and contained greater than 95% sand and less than 5% silt and clays. The majority of the sediment fell in Phi class of 3 to 1 (125 to 500 μm).

The most outstanding visual features of the Waquoit Bay cores are their colors as noted by Charette and Sholkovitz (2002). They concluded that the dark red, yellow and orange colors of the Waquoit Bay cores were iron (hydr)oxide precipitates loosely bound to sand grains. The quartz grains had a colored veneer which is easily removed from the sediment surface upon shaking with water. Leaching in a strong (1.4 M) solution of hydroxylamine hydrochloride in 6 M HCl, a well-known reductant of amorphous and/or crystalline iron (hydr)oxides, stripped the quartz-rich sands of their unique color and left a tan colored beachlike sand. The color changes occurred over a transition zone of many tens of centimeters. Core 2 changed from gray to dark red at a depth of ~85 cm; approximately half of this core was dark red in color. Core 3 changed from gray to red to orange; the gray section was restricted to the top 30 cm of this 112 cm-long core. Core 5 changed from gray to yellow, with the transition to yellow occurring 15 cm below the top of the core.

Linear combination Fe EXAFS fits of the Fe (hydr)oxide-coated sands confirm that there is a large diversity in the type of iron (hydr)oxides minerals being precipitated in closely spaced cores at the head of the Bay (Charette and Sholkovitz, 2002). The red coating of core 2 consisted predominantly of ferrihydrite (64%) with 26% goethite and 10% lepidocrocite. The yellow coating of core 5 contained 65% goethite and 35% ferrihydrite. The orange coating of core 3 consisted of all three forms of oxides at significant levels. It had the largest amount of lepidocrocite (19%), and goethite and ferrihydrite represent 44 and 37% respectively. The visual observations and the LC-EXAFS data for the Waquoit Bay cores are consistent with many studies of natural sediments which show that different colors broadly correspond to different structural forms of iron (hydr)oxide precipitates (Cornell and Schwertmann, 1996).

The organic matter content of the sandy sediments of Waquoit Bay is expectedly low relative to fine-grained marine sediments (electronic annex). The organic carbon concentration of the upper sediments range from 0.05 to 0.075% while the deep sediments contain undetectable to 0.015% organic C. Hence, there is a very small downcore decrease within an overall matrix of low organic content.

4.3. Total Oxide Concentrations

The data from elemental analyses of the three cores can be obtained from electronic annex. As discussed in section 3.2, the elemental concentrations in this article are derived from the two chemical leaches − L3 solution to dissolve "amorphous (hydr)oxides of iron and manganese" and L4 solution that targets "crystalline Fe and Mn (hydr)oxides." This section describes the sum of the L3 and L4 (L3 + L4) concentrations or the "total oxide" concentrations.

The main feature in Fe profiles is that all three cores have extensive downcore enrichments (Figs. 3–5). The offsite beach sand and the beach sand from Waquoit Bay contain only 200–300 ppm of Fe. In contrast, the total Fe in core 2 reaches values ~ 3500 ppm in the deepest section; a 2000 ppm increase between 80 to 120 cm coincides with the visually observed transition into the zone of red colored (ferrihydrite) iron (hydr)oxides. Core 3 contains the largest and the most continuous downcore increase in total oxide Fe concentration with values reaching ~7600 ppm Fe at 100 cm. Its large downcore increase at 40 cm coincides with the visually observed transition from gray to red/orange. The total Fe concentration of core 5 reaches ~3500 ppm at 170 cm. The largest gradient occurs between 30 and 60 cm where the yellow color becomes firmly established. This core contains more downcore scatter in composition and color than the other two cores.

The total [L3 + L4] Mn oxide concentration in cores 2, 3 and

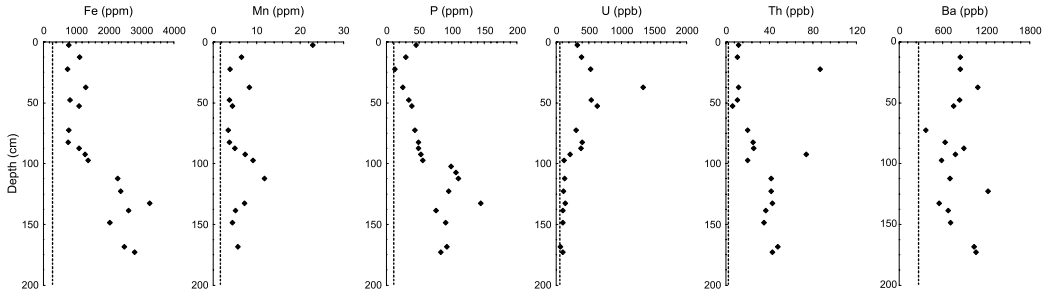

Fig. 3. Downcore distribution of total [L3 + L4] Fe, Mn, P, U, Th, and Ba concentrations in core 2. The dashed line indicates the background concentration of the element from sands collected at an offsite location.

5 ranges from 4 to 27 ppm (Figs. 3–5). Maximum Mn concentrations are 12, 27 and 14 ppm respectively. The average Fe/Mn [ppm/ppm] ratios of core 2, 3 and 5 are 264, 221 and 266 respectively. Hence, the concentration of amorphous plus crystalline Fe (hydr)oxides is more than two orders of magnitude larger than their Mn oxide counterpart. While total Mn (hydr)oxides are significantly less abundant than total Fe (hydr)oxides, the Mn profiles in cores 2 and 3 have well developed midcore maxima centered at 110 and 80 cm respectively. There is more scatter associated with the maximum at 50 cm in core 5. The peak (maximum minus baseline) Mn concentration of 20 ppm in core 3 is the highest of the three cores. Cores 2 and 5 had elevated concentrations of only 8–10 ppm.

The vertical profiles of [L3 + L4] P in cores 2, 3 and 5 have been discussed in Charette and Sholkovitz (2002). Offsite beach sand and beach sand from Waquoit Bay contain 10–12 ppm of [L3 + L4] P. In contrast, the Fe (hydr)oxide-rich deep layers of cores 1 and 3 are enriched and contain up to 100–200 ppm P. Core 5 has a significantly smaller maximum P (50 ppm). Cores 2 and 3 exhibit the most systematic downcore enrichments of P, while core 5 had considerable downcore scatter.

The downcore distributions of [L3 + L4] U and Th concentrations are distinctly different from each other − U enrichment in the upper portions and Th enrichment in the iron (hydr)oxide enriched deeper zones (Figs. 3–5). Cores 2 and 5 are characterized by well-developed subsurface concentration maxima of (L3 + L4) U. These values reach ~1300 and 1900 ppb between 30 and 60 cm. The baseline U concentrations above and below the maxima in core 2 are ~300 and 70 ppb respectively. Baseline concentrations in core 3 are 100 and 70 ppb. The (L3 + L4) U concentrations of the offsite beach sand and the beach sand at Waquoit Bay location are low (66 and 45 ppb, respectively). Hence, U enrichments are pronounced features in their upper zones of cores 2 and 5. In contrast, the [L3 + L4] U concentration in core 3 is generally invariant throughout the profile (240 to 420 ppb) and is 1.5 and 5

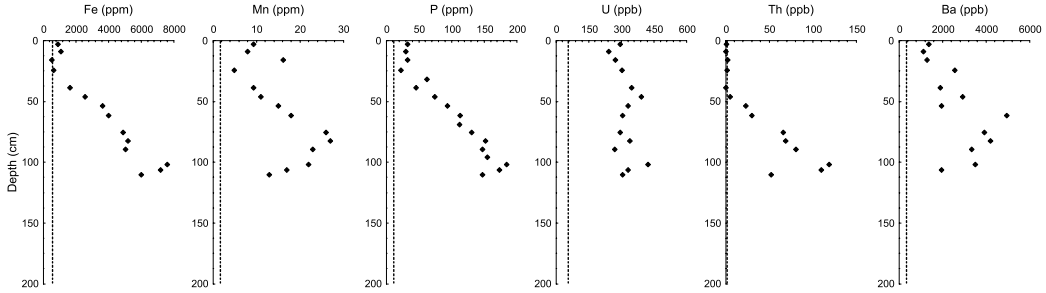

Fig. 4. Downcore distribution of total [L3 + L4] Fe, Mn, P, U, Th, and Ba concentrations in core 3. The dashed line indicates the background concentration of the element from sands collected at an offsite location.

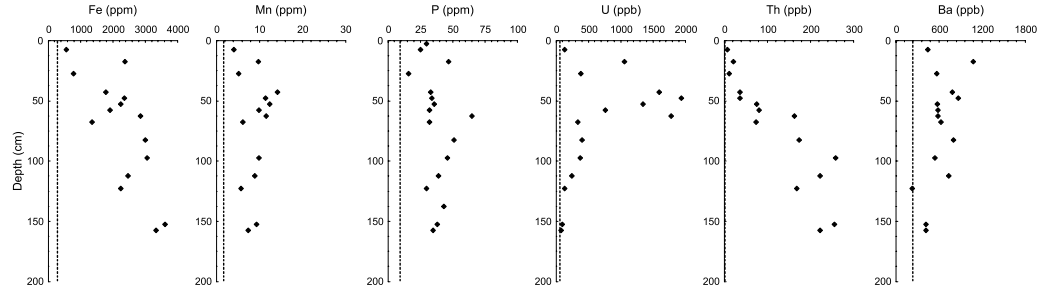

Fig. 5. Downcore distribution of total [L3 + L4] Fe, Mn, P, U, Th, and Ba concentrations in core 5. The dashed line indicates the background concentration of the element from sands collected at an offsite location.

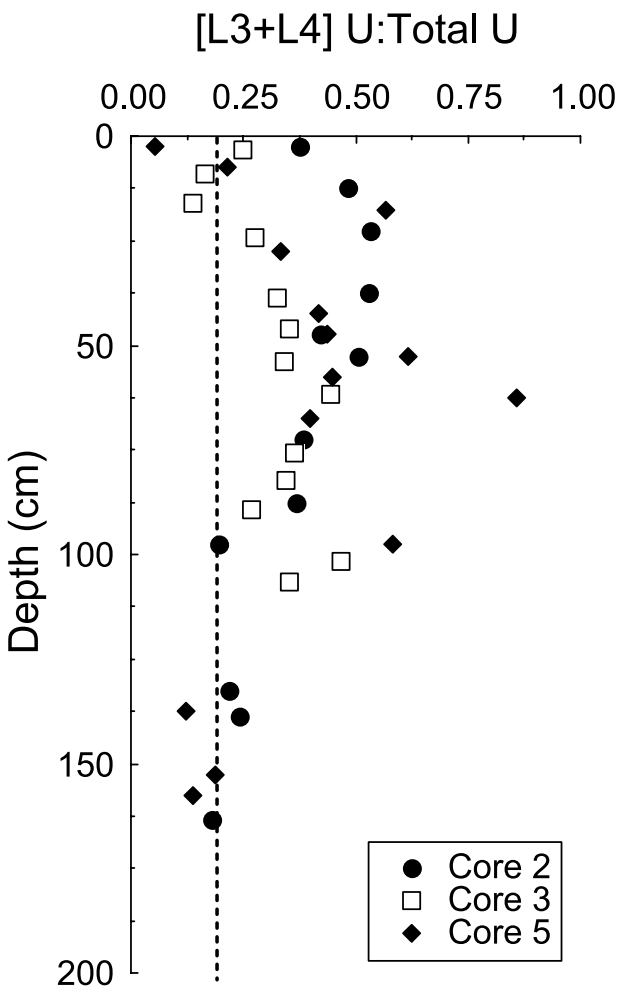

Fig. 6. Downcore distribution of the ratio of Fe (hydr)oxide-associated U vs. total U in cores 2, 3, and 5. Also shown is the ratio from the sands collected at an offsite location (dashed line).

times lower than in core 2 and 5 respectively. The core 3 concentrations are still significantly higher than the 70 ppb baseline levels deep in cores 2 and 5.

The ratio of (L3 + L4) U to γ-derived total U as a function of depth is compared in Figure 6. The surface (< 15 cm) and iron (hydr)oxide rich deep (> 120 cm) zones of cores 3 and 5 have a ratio of 0.18 (ppb/ppb) which is similar to the ratio of the offsite beach sand. However, the upper 100 cm of all three cores have broad subsurface maxima in the (L3 + L4) U/(total gamma U) ratio; values range from 0.40 to 0.86. Hence, the proportion of chemically leached U is highest in the upper zones of the cores where the both (L3 + L4) U and total gamma U concentrations reach their highest levels. In contrast, the majority of U in the iron (hydr)oxide rich deeper zones exists in the nonleachable fraction of the sediments (Fig. 6).

With respect to Th content, all three cores are characterized by low [L3 + L4] concentration (< 12 ppb) in the upper 25 to 50 cm, followed by a steady increase with depth (Figs. 3–5). The Th concentrations in the deepest horizons of cores 2, 3 and 5 reach 50, 120 and 250 ppb respectively. Offsite beach sand and beach sand from Waquoit Bay have low (≤ 3 ppb) Th contents. Th enrichment coincides with the iron (hydr)oxide enriched deep zones of the three cores.

The [L3 + L4] Ba concentrations in cores 2, 3 and 5 are appreciably higher than in the offsite beach sand and the beach sand at Waquoit Bay (445 and 232 ppb, respectively) (Figs. 3–5). The highest concentrations in cores 2 and 5 reach ~1100 ppb. In contrast, core 3 has four times that value (4900 ppb Ba at 62 cm); it also has a well-developed subsurface Ba maxima, with concentrations increasing from 1100 to 1300 ppb in the upper layers to 3900–4900 ppb in the 60–80 cm region before decreasing to 1900 ppb at 106 cm. The Ba profile of core 3 is similar to that of Mn, which is also characterized by a well-developed subsurface maximum in the same region of the profile.

4.4. Elemental Concentrations in the Amorphous and Crystalline Oxides

The distribution of the elements between the amorphous (L3 leach) and crystalline oxides (L4 leach) are briefly described in this section. The L3 and L4 concentrations of Fe and P in cores 2 and 3 increase with depth in a manner similar to their total oxide concentrations (Figs. 3–5); they also show a fairly equal downcore distributions of between the amorphous and crystalline oxides (Fig. 7). The partitioning of Fe and P in the core 5 differs dramatically in that the downcore increases in total oxide concentrations of Fe and P are predominately associated with the crystalline oxides (L4 leach).

U and Th exhibit significantly different partitioning with respect to each other and to the Fe (hydr)oxides fractions. The large enrichment of total oxide U in the upper 50 cm of cores 2 and 5 is mostly (> 85%) associated with the amorphous oxides (L3; Fig. 7), while the enrichment of total oxide Th in cores 2, 3 and 5 below 50 cm (Figs. 3–5) is predominately (>75%) associated with the crystalline oxides (L4; Fig. 7).

Only core 3 has a well-developed maximum in the total oxide concentrations of Mn and Ba (Fig. 4). While Mn is fairly equally distributed between the amorphous and crystalline oxides, the Ba maximum is associated predominately with the amorphous oxide (L3). Mn and Ba show no distinct features in the L3 and L4 fractions of cores 2 and 5.

5. DISCUSSION

5.1. Hydrogeochemical Model

The schematic diagram in Figure 8 will be used as a template for discussing the geochemical cycles within the Waquoit Bay sediment. This figure incorporates the hydrology of the subterranean estuary and the trends we observed in the downcore distributions of Fe, Mn, P, U, Th and Ba. Briefly, a plume of seaward flowing fresh groundwater and recirculating seawater (Cooper, 1959; Ataie-Ashtiani et al., 1999; Li et al., 1999) lead to a salt-wedge type distribution of pore-water salinity (Fig. 2). The sedimentary and aqueous environment of this subterranean estuary is one of active redox reactions for Fe and Mn. There are two distinct sources of soluble and reduced Fe and Mn. One source resides in the upward rising plume of freshwater, and the second source lies in the salt-wedge zone of mid- to high-salinity pore waters (Fig. 2). The latter source lies directly below the sediment cores containing high concentrations of

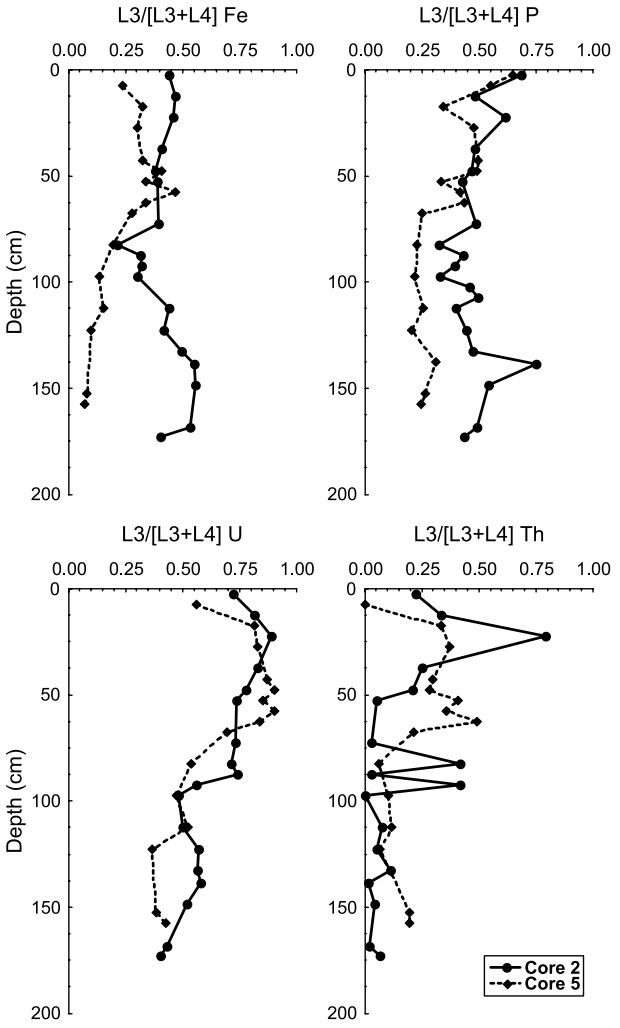

Fig. 7. Downcore distribution of total [L3 + L4] Fe, P, U, and Th concentration associated with the L3 leach for cores 2 and 5.

iron (hydr)oxide precipitates. Circulating seawater transports dissolved U and Ba to the sediments. Uranium removal occurs in the upper zone of reducing sediments and Ba enrichment is more closely associated with the formation of Mn (hydr)oxides. The basis for these observations is discussed in the following sections.

5.2. Oxides of Fe and Mn

Charette and Sholkovitz (2002) attributed the formation of iron (hydr)oxide rich sands at the head of the bay to the oxidation of ferrous iron derived from terrestrial groundwater. The pore-water profiles reveal a more complex picture of the redox-driven processes and sources of reduced iron. As shown in Figure 2, there is a seaward-moving plume of ferrous-rich groundwater that has a terrestrial source. A major fraction of the ferrous iron is oxidized within the freshwater end of subterranean estuary between piezometers 6 and 3 (Fig. 2). This observation suggests that the sediments at the leading edge of the freshwater plume should contain large amounts of iron (hydr)oxides. Indeed, pore water pumped from piezometer 3 at a depth of ~3 m contained suspended yellow particles that are nearly pure iron (hydr)oxides. The act of pumping presumably resuspended the oxides off the sands.

The salt-wedge section of the subterranean estuary also contains elevated concentrations of pore-water Fe (Fig. 2). This large reservoir of reduced and dissolved Fe underlies the iron-oxide rich sediments of cores 2, 3 and 5. The sharp decrease in pore-water Fe between 4 m and 2 m in piezometer 5 suggests that the oxidation of reduced Fe to iron (hydr)oxide is occurring. Seepage meter studies in this same region of Waquoit Bay have shown that subterranean circulation leads to the upward flow of saline pore water to the intertidal zone (Michael et al., 2003; Sholkovitz et al., 2003). Hence, the pore-water profiles reveal that there are two major sources and oxidative sinks of reduced iron in Waquoit Bay. The upward transport and oxidation of Fe(II)-rich pore waters from saline zone represents one potential source of the iron (hydr)oxide rich cores reported in Charette and Sholkovitz (2002). A freshwater plume from the land also transports high concentrations of dissolved Fe(II) toward the bay where the precipitation of iron (hydr)oxides occurs in the freshwater end of the plume. These terrestrial and marine sources are probably interconnected as they operate within several meters of each other in the vertical and offshore directions. Though the pattern of recharge to the aquifer follows a seasonal cycle (~0.75 m amplitude ~1 km inland; USGS well 413525070291904), it is unclear how exactly this translates to movement of the salt wedge in the subterranean estuary. However, it is likely that hydrologic cycles have some effect on the extent and location of the iron (hydr)oxide rich sands. Given that we only present groundwater profiles and sediment cores collected during a single time point, we are unable to quantify what effect this might have. In either case, terrestrial groundwater is probably the ultimate source of "new" Fe to the permeable sediments of this coastal aquifer.

If we assume that the fresh groundwater Fe plume is the primary source of Fe(II) for the iron (hydr)oxide rich sediments, then what time-scale would be required to create the observed Fe enrichments in the sediment? Given the Abraham et al. (2003) estimate of groundwater discharge for the head of Waquoit Bay (0.08 m d^{-1}), a typical groundwater Fe concentration of 100 μM, we estimate the Fe accumulation rate in this zone to be 8 mmol Fe m^{-2} d^{-1}; this calculation assumes that all of the dissolved Fe is oxidized within the subterranean estuary and therefore not discharged into the Bay. Then, using a conservative sediment Fe concentration of 3000 ppm, an assumed sediment density of 2 g cm^{-3}, and an iron-rich zone that is 2 m deep, we estimate the sediment inventory of Fe to be 210 mol Fe m^{-2}. Given the estimated groundwater Fe flux rate, it would take ~72 yr to accumulate the observed sediment Fe inventory level. Future studies of this system will examine the seasonal and interannual dynamics of the Fe plume and iron (hydr)oxide rich sediments and as a result will be more poised to address the key questions relating to the dynamics of the geochemical cycles in this system.

Elevated concentrations of dissolved Mn are also signature features of the freshwater plume and the saline groundwater of the subterranean estuary (Fig. 2). The one prominent difference between the distributions of Mn and Fe in the salt wedge section is that the mid-depth maximum in pore-water Mn lies above the zone of high pore-water Fe. This vertical offset of 2

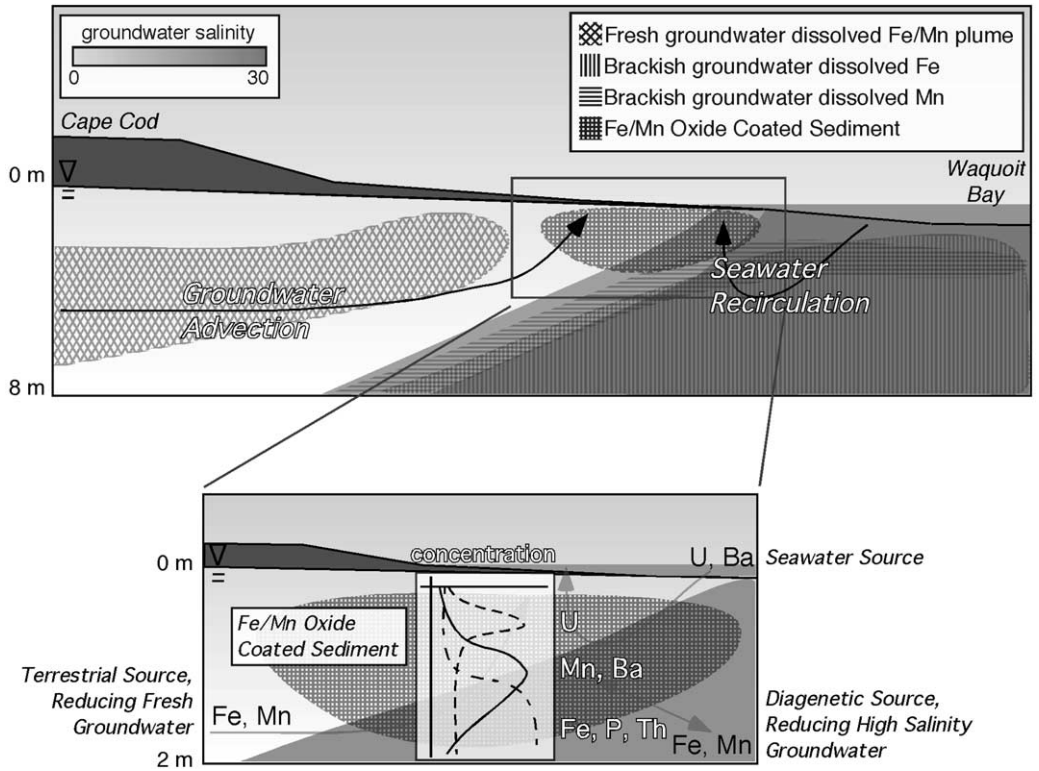

Fig. 8. Schematic diagram of a cross-section through the subterranean estuary providing an overview of the major hydrogeologic and geochemical processes discussed in this article.

to 3 m is seen most clearly in piezometers 6, 3 and 5 Fe (Fig. 2). With respect to the sedimentary composition, the total oxide concentrations of Mn and Fe in cores 2 and 3 also displayed differences in their downcore distributions (Figs. 3-4). Specifically, the Mn concentration has a midcore maximum while Fe concentrations generally increased with depth.

These differences in both the pore water and sediment profiles of Fe and Mn of Waquoit Bay are consistent with the well-established depth sequence of redox reactions in marine sediments (e.g., Froelich et al., 1979; Aller, 1980; Burdige, 1993). Redox-driven stratification of Fe and Mn, of the type presented here for the Waquoit Bay subterranean estuary, is also observed in the water column of marine anoxic basins and surface estuaries where strong salt gradients separate oxic from anoxic waters (e.g., Lewis and Landing, 1991). Briefly, large differences in their rates of oxidation and reduction lead to the preferential oxidation of dissolved Fe(II) to Fe(III) oxides and the preferential reduction of Mn(IV) oxides to dissolved Mn(II) (Stumm and Morgan, 1981). These differences in redox properties lead to fractionation process whereby Mn (hydr)oxides are formed at shallower depths than iron (hydr)oxides. High concentrations of dissolved Mn(II) and particulate Mn(IV) oxides typically overlie their iron counterparts in anoxic basins and marine sediments (Aller, 1980; Thamdrup et al., 1994; Slomp et al., 1997).

The Mn oxide content of the cores are two orders of magnitude less abundant that their iron (hydr)oxide counterparts. The saline pore water has similar concentrations of Mn (40 μM) and Fe (50 μM), while the fresh pore-water plume has a Fe/Mn ratio of $\sim$10. This difference most likely reflects differences in the sediment types and in the diagenetic reactions of the freshwater and marine sections of the aquifer. However, given that the Fe/Mn ratio of the sediments is high as well, the elevated dissolved Mn in the saline pore water may also reflect the fact that Mn has a significantly longer residence time relative to dissolved Fe in aquatic systems (Stumm and Morgan, 1981).

One outstanding feature of the Waquoit Bay system is the large variability in the type of iron (hydr)oxides contained in closely spaced cores (Charette and Sholkovitz, 2002). The red coating of core 2 consisted predominantly of ferrihydrite (80%) with 10% each of goethite and lepidocrocite. The yellow coating of core 5 contained 61% goethite and 39% ferrihydrite and the orange coating of core 3 consisted of lepidocrocite (19%), goethite (31%) and ferrihydrite (50%). At this stage, our data cannot offer the geochemical reasons behind this diversity at the scale of only tens of meters. However, studies of iron (hydr)oxide formations have shown that mineral forms can be controlled by variety of environmental factors; these include salinity, dissolved concentrations of sulfate and silica, pH and age (Carlson and Schwertmann, 1981; Cornell and Schwertmann, 1996; Mayer and Jarrell, 1996; Larson and Postma, 2001). Microbial activity likely plays a major role in the oxidation and reduction of Fe and Mn and in the formation of different oxide types (e.g., Lovely and Phillips, 1986; Canfield, 1989; Lovely, 1991; Burdige, 1993; Emerson and Moyer, 1997; Zachara et al., 2001).

5.3. Organic Matter and Redox Conditions

Waquoit Bay sediments are low in organic carbon as expected for permeable beach sands. However, the beach and intertidal areas at the head of Waquoit Bay have a dense coverage of green and brown algae in the late spring and summer. Hence, there is a large production of biodegradable organic matter in the warm months of the year. Because our cores were collected at the end of the winter (April 2001), the organic carbon concentrations in the surface sediments were probably at an annual low.

One mechanism for the downward transport of particulate organic material in permeable sediments is the action of waves and tides on porous beach sands (Huettel et al., 1996; Huettel and Rusch, 2000; Rusch and Huettel, 2000). Huettel et al. (1996) reported that the transport depths by these mechanisms are fairly shallow (< 10 cm). Though we have no information regarding the quantity of the annually produced organic matter that might get transported down into the Waquoit Bay sediments via this mechanisms, the downcore decrease in organic carbon suggests 20–50 cm as a maximum depth of transport (electronic annex). A second possibility is seawater circulation through the sediments of the subterranean estuary driven by a combination of tidal effects and groundwater discharge to the bay (Ataie-Ashtiani et al., 1999). This circulation pattern could transport reactive organic matter in the form of small particles and dissolved organic matter to the deep sections of our cores and pore-water profiles. Organic matter in the freshwater plume might represent another source of organic matter to the top of the subterranean estuary. This water has a fairly high concentration of dissolved organic carbon (> 200 μM).

Despite the low concentrations of organic carbon in the Waquoit Bay sediments, all of our observations point to active microbial biodegradation of organic matter and active Fe/Mn redox cycles in the permeable sediments at the head of Waquoit Bay. This same conclusion was reached by other groups studying the biogeochemistry of beach faces and shelf sands (Huettel et al., 1998; Huettel and Rusch, 2000; D'Andrea et al., 2002; Ullman et al., 2003; Windom and Niencheski, 2003). They note that these environments have high turnover rates of diagenetically reactive organic matter and nutrient remineralization.

5.4. Sorption of P onto Fe (Hydr)Oxides

Phosphate is known to strongly adsorb onto naturally occurring Fe (hydr)oxides (e.g., Borggaard, 1983; Parfitt, 1989; Torrent et al., 1992; Griffieon, 1994). With the notable exception of core 5, the P/Fe [L3 + L4] ratios of cores 2 and 3 fall within a fairly narrow range which is similar to those observed in iron (hydr)oxides at other coastal sediments (Fig. 9; Charette and Sholkovitz, 2002, and references therein). The P/Fe ratios of the iron-rich deep sections of core 5 are 1.5 to 2.7 times lower than in the other cores (Fig. 9). The yellow-colored oxide of core 5 is unique amongst the cores in that it contained a much higher abundance of goethite (61% vs. 10% in core 1 and 31% in core 2). Slomp et al. (1996) argued that goethite-rich sediments have less Fe-bound P due to the reduced affinity of P for this more crystalline form of iron (hydr)oxide. Charette and Sholkovitz (2002) invoked this observation to explain the lower P/Fe ratios of the core 5 oxides. This explanation is

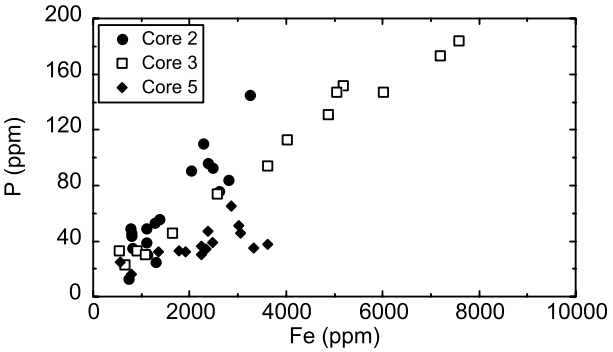

Fig. 9. Total [L3 + L4] Fe vs. P in cores 2, 3 and 5.

further supported by the elemental partitioning between the L3 and L4 solutions, which show that Fe and P in core 5 were preferentially (~75%) associated with the more crystalline form (L4) of the oxides (Fig. 7). This is not the case for cores 2 and 3 where the Fe and P are fairly equally distributed between the amorphous (L3) and crystalline (L4) forms of the oxide. Hence, the more crystalline form of iron (hydr)oxide in core 5 appears to significantly decrease the P/Fe ratio.

5.5. Uranium Enrichment

Geochemists have long recognized that uranium enrichment is a robust indicator of reducing marine sediments (e.g., Veeh, 1967; Mo et al., 1973; Klinkhammer and Palmer, 1991). Boundaries or fronts between oxidizing and reducing sediments are also sites of U enrichment (Colley and Thomson, 1985). Hence, U enrichment in the Waquoit Bay sediments is strong evidence for reducing conditions in the near-surface sediments (Figs. 3–6). This redox stratigraphy, whereby reducing conditions overlie oxidizing conditions, is upside down with respect to the "normal" sequence in fine grained marine sediments where downcore redox conditions go from oxidizing toward reducing.

As noted in section 4.3, both the nondestructive gamma counting technique and the chemical (L3 + L4) leaching technique have revealed coincident U enrichments in the upper region of cores 2 and 5. (The former technique also reveals a small enrichment in core 3 that is not evident with the leach data (Fig. 6)). In addition, most of the U (>75%) in this U-enriched layer is associated with the amorphous (L3) iron (hydr)oxide fraction (Fig. 7). This dual observation of U enrichment suggests that the (L3 + L4) U data are not necessarily artifacts of leaching. Given that U in natural waters and sediments has an active redox chemistry and several redox species, the interpretation of the L3 and L4 data are less straight forward than with nonredox elements such as P and Th. For example, the hydroxylamine hydrochloride component of the L3 and L4 solutions is a strong reductant that could reduce all the ambient U(VI) in the sediments to U(IV). If this transformation occurred in the leaching steps, then it would yield a less soluble U species and large artifacts in our downcore distributions of (L3 + L4) U. While we do not have any information with respect to how the L3 and L4 solutions modify the redox state of U in our sediments, the γ-derived enrichments argue that the

chemical leaching technique is recording U enrichment in the upper sediment.

Abiotic and biotic reduction of U(VI) to U(IV) are well documented processes in natural waters and sediments (e.g., Church et al., 1981; Cochran et al., 1986; Anderson et al., 1989a,b; Lovely et al., 1991; McKee and Todd, 1993; Liger et al., 1999; Fredrickson et al., 2000). These processes, used to explain the enrichment of U in reducing marine sediments, are most likely operating in the Waquoit Bay sediments. As noted in section 4.1, reducing conditions develop within the upper 50 cm of the Bay's intertidal zone as a result of algal matter decomposition. Hence, this zone support abiotic and/or biotic reduction of U(VI) from seawater. The strongest evidence for U removal comes from our pore-water data which show almost complete depletion of dissolved U at the high-salinity end of the subterranean estuary; our pore-water U data will be discussed in part 2 of this series of papers.

Why are the iron (hydr)oxide rich sediments, deeper in the cores, not accumulating U? The existence of Fe and Mn (hydr)oxides implies that the redox conditions are not conducive to the abiotic or biotic reduction of U(VI). While iron (hydr)oxides are known to be strong adsorbers of U in fresh water, this process is much less effective in oxic seawater where U(VI) is strongly complexed with carbonate ions (Hsi and Langmuir, 1985). Hence, the adsorption of U by iron (hydr)oxides should not be an important process in these cores, all of which come from the salty section of the subterranean estuary (Fig. 2).

In summary of this subsection, the subterranean estuary in Waquoit Bay is the site of an active redox cycle for U. The recirculation of seawater continuously pumps in soluble U(VI) to reducing sediments in the upper zone of the cores. This source, coupled with the abiotic and/or biotic reduction of soluble U(VI) to insoluble U(IV), leads to the U enrichments (Fig. 3–7). Anderson et al. (1989b) and Shaw et al. (1994) have shown that the exposure of reducing marine sediments to oxic seawater leads to the release of dissolved U. This implies that U might be released to the water column of Waquoit Bay in the winter months when the reducing surface sediments of summer are oxidized.

5.6. Th Enrichment

Thorium enrichment in the deeper sections that contain Fe (hydr)oxide rich sand is a feature of all three cores. The strong relationship between the (L3 + L4) concentrations of Th and Fe (Fig. 10) is consistent with the fact that iron (hydr)oxides are strong adsorbers of Th in seawater (Bacon, 1988; Hunter et al., 1988). Core 5 had significantly higher concentrations of Th and higher Th/Fe ratios than the other two cores (Fig. 10). The averaged Th/Fe (ppb/ppm) ratio for sediment deeper than 47 cm in core 5 is 0.063. This ratio in core 2 (> 53 cm) and core 3 (> 52 cm) is 0.018 and 0.012 respectively. These observations appear to be inconsistent with our previous argument that the more crystalline goethite (61% of the iron (hydr)oxides in core 5) had less sorption affinity for P. One would expect that goethite, with its more crystalline form and its smaller surface area to weight ratio, would adsorb less Th than the ferrihydrite-rich (80%) core 2. Goethite, in fact, may have a stronger affinity for Th than the less crystalline forms of iron (hydr)oxides. During the aging of hydrous iron (hydr)oxides, Ford et al. (1997) noted that different metals behaved differently as ferrihydrite transformed into goethite. Specifically, Mn(II) and Ni(II) increased their apparent sorption while Pb(II) and Cd(II) displayed net desorption. They concluded that this difference was consistent with the different structural properties of the iron (hydr)oxides. Dardenne et al. (2002) reported that the lanthanide Lu changed from being reversibly bound to being more strongly bound as ferrihydrite aged to hematite. Such a process may explain why the major fraction of total Th in all three cores is associated with the crystalline (L4) oxides and not amorphous (L3) oxides (Fig. 7).

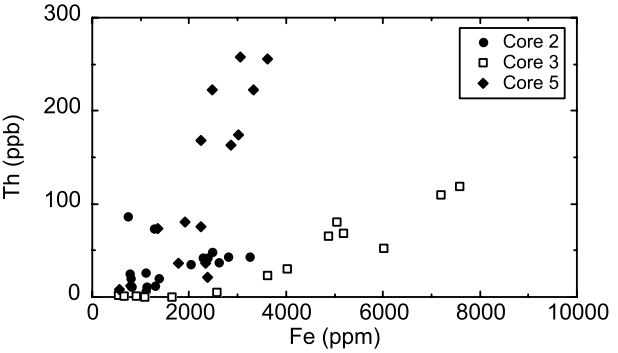

Fig. 10. Total [L3 + L4] Fe vs. Th in cores 2, 3 and 5.

5.7. Ba Sorption to Fe and Mn (Hydr)Oxides

Core 3 stands out from the other cores in having both the highest (L3 + L4) Ba concentrations and a well developed subsurface Ba maximum between 60 and 80 cm (Fig. 4). This core also contains the highest concentrations of Mn oxide and a subsurface maximum, which tracks that of Ba. While core 3 also has the highest Fe (hydr)oxide concentrations of all the cores, the Fe profile is one of a continuous downcore increase through the zone of Mn and Ba maxima. Although it is difficult to use relationships of sediment concentrations to draw conclusions about geochemical processes, the correlation between Mn and Ba in core 3 (R_2 = 0.45) is stronger than correlation between Fe and Ba (R_2 = 0.31) (Fig. 11). In contrast, these same pairs of elements are weakly correlated in cores 2 and 5 (Figs. 3, 5 and 11). Even though Mn (hydr)oxides are 200–300 times less abundant than Fe (hydr)oxides in core 3, Mn (hydr)oxides have an affinity for Ba which is many orders of magnitude greater than iron (hydr)oxides (Balistrieri and Murray, 1986; Sugiyama et al., 1992; Mishra and Tiwary, 1993). Ingri and Ponter (1986), for example, noted a strong correlation between Ba and Mn in Gulf of Bothnia sediment that contains layers of both Fe and Mn (hydr)oxides. Hence, the downcore distribution of Ba in the Fe (hydr)oxide rich sediments of core 3 is most probably controlled by the presence of Mn (hydr)oxides. This leads to the conclusion that the release of dissolved Ba in subterranean estuaries may be partially explained by the reductive dissolution of Mn (hydr)oxides (Fig. 8).

The traditional view has been that Ba release in estuaries and brackish pore water is controlled primarily by ion exchange (e.g., Li and Chan, 1979; Shaw et al., 1998). However, the distribution of pore-water Ba, presented in part 2 of this series

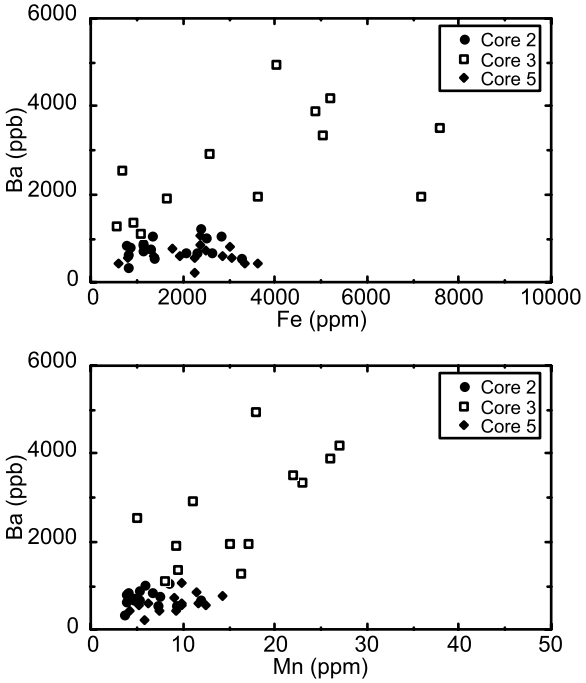

Fig. 11. Total [L3 + L4] Fe vs. Ba and Mn vs. Ba in cores 2, 3 and 5.

of articles on the Waquoit Bay subterranean estuary, will show that Ba concentrations are greatly elevated in the zone of elevated Mn concentrations and intermediate salinity (Fig. 2). The sediment results in combination with the pore-water data suggests that Ba release associated with reductive dissolution Mn hydr(oxides) may be important as well.

6. CONCLUSIONS

Sediment cores were collected from the head of Waquoit Bay (Cape Cod, MA, USA) where groundwater mixes with seawater in highly permeable sediments to form a well-defined subterranean estuary. Though the concentrations of organic carbon in the Waquoit Bay sediments are low, all of our observations point to active microbial biodegradation of organic matter and active Fe/Mn redox cycles in this coastal aquifer. The deeper sections of the cores are characterized by large amounts of iron (hydr)oxides (ferrihydrite, lepidocrocite and goethite) that are being precipitated onto organic C-poor quartz sand. Unlike Fe (hydr)oxides which increase with depth, the Mn (hydr)oxides display well-developed maxima in the midsections of cores 2 and 3. This type of vertical stratification is consistent with redox-controlled diagenesis in which Mn (hydr)oxides are formed at shallower depths than iron (hydr)oxides. The reduction of seawater-derived sulfate and the production of sulfides are not important parts of the redox-driven cycles in this system.

Groundwater delivers high concentrations of dissolved ferrous iron and reduced manganese to the freshwater end of the subterranean estuary where a large fraction of this dissolved Fe and Mn is oxidizatively precipitated onto the sands. Density stratification, driven by a strong salinity-controlled pycnocline, leads to diagenetically-produced reducing conditions and high concentrations of pore-water Fe and Mn in the mid- to high-salinity region of the subterranean estuary. The advective transport and subsequent oxidation of this Fe and Mn is responsible for the formation of iron (hydr)oxide rich sands at the high-salinity end of Waquoit Bay's subterranean estuary.

A selective dissolution method was used to measure the concentrations of P, Ba, U and Th that are associated with "amorphous (hydro)oxides of iron and manganese" and "crystalline Fe and Mn (hydr)oxides." The concentrations of these elements display distinctive downcore distributions in response to the redox properties of the sediments. P and Th are enriched in the deep sections of the cores where Fe (hydr)oxides are the dominant diagenetic phase. The strong association of P and Th with Fe (hydr)oxides is consistent with their known geochemical (adsorption) properties. Even though Mn (hydr)oxides are 200–300 times less abundant than Fe (hydr)oxides, the midcore maximum in Ba in core 3 is likely caused by the preferential adsorption of Ba onto the oxides of Mn whose affinity for Ba is many orders of magnitude greater than that of iron (hydr)oxides. The enrichment of U in the upper zones of the cores is consistent with the formation of reducing conditions in near-surface sediments at the head of the Bay, following the production of algae in the late spring and summer. The accumulation of surface bound U in the upper sediments is caused by abiotic and/or biotic reduction and removal of U(VI) from seawater. Hence, the recirculation of seawater through this type of subterranean estuary can act as net sink of Ba and U from seawater (Fig. 8).

The amorphous fraction is correlated closely with the amount of ferrihydrite present in the sands while a greater goethite/lepidocrocite component explains a more equal amorphous vs. crystalline distribution of total Fe (hydr)oxides. The more reactive/bioavailable ferrihydrite fraction has a higher affinity for P, as evidenced by the P/Fe ratio differences between cores 2 and 5. In contrast, the more aged goethite/lepidocrocite minerals, as result of their more crystalline structure and incorporation of foreign ions within the (hydr)oxides, are less reactive with respect to elements with an affinity for Fe (hydr)oxides. In the intermediate-depth U enriched fractions of the core, U is very strongly associated with the amorphous (hydr)oxide fraction, which supports the concept that U is recently removed to the sediments via seawater circulation. Finally, it is likely that elements such as Th have a higher affinity for the more crystalline (hydr)oxides. Alternatively, during ripening of the amorphous (hydr)oxides, Th could be incorporated into the structure of the more crystalline (hydr)oxides. Hence, the form (and not only the quantity) of iron (hydr)oxides plays an important role in how elements are cycled in permeable sediments.

Coastal aquifers with groundwater flow and subterranean estuaries are common along the eastern coast of the United States (USGS, 2003) and in other parts of the world's coastline where sand deposits exist (Burnett et al., 2001, 2002). As shown with the Waquoit Bay system, the formation of iron and manganese rich sands requires a freshwater aquifer with dissolved Fe(II) and Mn(II) that out crops into oxygenated coastal sediments and/or redox-driven diagenesis within sandy coastal deposits. These two hydrogeochemical conditions may not be uncommon as exemplified by the studies of Huettel et al. (1998) on the sandy beaches of the German North Sea. Their

field observations and flume experiments show that the active biogeochemistry occurs in the intertidal zone. This includes the formation of iron (hydr)oxides as reducing pore water is advected to the surfaces of their beach sands and ferrous iron oxidizes. Iron (hydr)oxide formation also occurs on the sandy beaches of coastal New York (Montlucon and Sanudo-Wilhemey, 2001). Sandy shelf sediments, low in organic matter, can also support redox cycles of Fe and Mn in the Baltic region (Kristensen et al., 2002). Sandy beach face sediments in Delaware, also low in organic matter, support nutrient remineralization within a freshwater-seawater system of a subterranean estuary (Ullman et al., 2003). As the sediment and pore-water composition of coastal aquifers become better documented, the Fe and Mn redox-dominated biogeochemistry of the Waquoit Bay system will be less unique.

Acknowledgments—We thank Craig Herbold, Matt Allen and Adam Rago for their help in the field and in the laboratory. Lary Ball and David Schneider of the WHOI ICP-MS Facility performed the trace metal analyses. Larry Poppe and Flavia Wood of the USGS Woods Hole Science Center conducted the grain-size analysis. X-ray absorption spectroscopy was carried out at the Stanford Synchrotron Radiation Laboratory, a national user facility operated by Stanford University on behalf of the U.S. Department of Energy, Office of Basic Energy Sciences. The SSRL Structural Molecular Biology Program is supported by the Department of Energy, Office of Biologic and Environmental Research, and by the National Institutes of Health, National Center for Research Resources, Biomedical Technology Program. We extend our continued appreciation to the director and staff of the Waquoit Bay National Estuarine Research Reserve for allowing and encouraging us to use Waquoit Bay as our study site. Finally, we thank Tim Shaw and two anonymous reviewers for their comments, which greatly improved the manuscript. This research was supported by the National Science Foundation (OCE-0095384) to M.A.C. and E.R.S., and a WHOI Coastal Ocean Institute Fellowship to M.A.C. This article is WHOI Contribution No. 11240.

Associate editor: T. Shaw

REFERENCES

Abraham D. R., Charette M .A., Allen M. C., Rago A., and Kroeger K. D. (2003) Radiochemical estimates of submarine groundwater discharge to Waquoit Bay, Massachusetts. *Biol. Bull.* **205,** 246–247.

Aller R. C. (1980) Diagenetic processes near the sediment-water interface of Long Island Sound II. Fe and Mn. *Adv. Geophys.* **22,** 351–415.

Anderson R. F., Fleisher M. Q., and LeHuray A. (1989a) Concentration, oxidation state and particulate flux of uranium in the Black Sea. *Geochim. Cosmochim. Acta* **53,** 2215–2224.

Anderson R. F., LeHuray A. P., Fleisher M. Q., and Murray J. W. (1989b) Uranium deposition in Saanich Inlet sediments, Vancouver Island. *Geochim. Cosmochim. Acta* **53,** 2205–2213.

Ataie-Ashtiani B., Volker R. E., and Lockington D. A. (1999) Tidal effects on sea water intrusion in unconfined aquifers. *J. Hydrol.* **216,** 17–31.

Bacon M. P. (1988) Tracers of chemical scavenging in the ocean: Boundary effects and large-scale chemical fractionation. *Phil. Trans. R. Soc. Lond. A* **325,** 147–160.

Balistrieri L. S. and Murray J. W. (1986) The surface chemistry of sediments from the Panama Basin: The influence of Mn (hydr)oxides on metal adsorption. *Geochim. Cosmochim. Acta* **50,** 2235–2243.

Basu A. R., Jacobsen S. B., Poreda R. J., Dowling C. B., and Aggarwal P. K. (2001) Large groundwater strontium flux to the oceans from the Bengal Basin and the marine strontium isotope record. *Science* **293,** 1470–1473.

Borggaard O. K. (1983) The influence of iron (hydr)oxide on phosphate adsorption by soil. *J. Soil Sci.* **34,** 333–341.

Boyle E., Edmond J., and Sholkovitz E. R. (1977) Mechanisms of iron removal in estuaries. *Geochim. Cosmochim. Acta* **41,** 1313–1324.

Burdige D. J. (1993) The biogeochemistry of Mn and Fe reduction in marine sediments. *Earth Sci. Rev.* **35,** 249–284.

Burnett W. C., Taniguchi M., and Oberdorfer J. (2001) Measurement and significance of the direct discharge of groundwater into the coastal zone. *J. Sea Res.* **46,** 109–116.

Burnett W., Chanton J., Christoff J., et al. (2002) Assessing methodologies for measuring groundwater discharge to the ocean. *Eos* 83, 117, **122,** 123.

Cambareri T. C. and Eichner E. M. (1998) Watershed delineation and ground water discharge to a coastal embayment. *Ground Water* **36,** 626–634.

Canfield D. E. (1989) Reactive iron in marine sediments. *Geochim. Cosmochim. Acta* **53,** 619–632.

Carlson L. and Schwertmann U. (1981) Natural ferrihydrites in surface deposits from Finland and their association with silica. *Geochim. Cosmochim. Acta* **45,** 421–429.

Charette M. A., Buesseler K. O., and Andrews J. E. (2001) Utility of radium isotopes for evaluating the input and transport of groundwater-derived nitrogen to a Cape Cod estuary. *Limnol. Oceanogr.* **46,** 465–470.

Charette M. A. and Sholkovitz E. R. (2002) Oxidative precipitation of groundwater-derived ferrous iron in the subterranean estuary of a coastal bay. *Geophy. Res. Lett.* **29,** 10.1029/2001GL014512.

Church T. M., Lord C. J., and Somayajulu B. K. L. (1981) Uranium, thorium and lead nuclides in a Delaware salt marsh sediment. *Estuar. Coast. Shelf. Sci.* **13,** 267–275.

Cochran J. K., Carey A. E., Sholkovitz E. R., and Surprenant L. D. (1986) The geochemistry of uranium and thorium in coastal marine sediments and sediment pore waters. *Geochim. Cosmochim. Acta* **50,** 663–680.

Coffrey M., Dehairs F., Collette O., Luther G., Church T., and Jickells T. (1997) The behavior of dissolved barium in estuaries. *Estuar. Coast. Shelf Sci.* **45,** 113–121.

Colley S. and Thomson J. (1985) Recurrent uranium relocations in distal turbidities emplaced in pelagic conditions. *Geochim. Cosmochim. Acta* **49,** 2339–2348.

Cooper H.H. (1959) A hypothesis concerning the dynamic balance of fresh water and salt water in a coastal aquifer. *J. Geophys. Res.* **71,** 461–467.

Cornell R. M. and Schwertmann U. (1996) *The Iron (Hydr)Oxides.* VCH.

D'Andrea A. F., Aller R. C., and Lopez G. R. (2002) Organic matter flux and reactivity on a South Carolina sandflat: The impact of pore water advection and macrobiological structures. *Limnol. Oceanogr.* **47,** 1056–1070.

Dardenne K., Schafer T., Lindqvist-Reis P., Denecke M. A., Plaschke M., Rothe J., and Kim J. I. (2002) Low temperature XAFS investigations of lutetium binding changes during the 2-line ferrihydrite alteration process. *Environ. Sci. Technol.* **36,** 5092–5099.

Edmond J. M., Spivack A., Grant B. C., Ming-Hui H., Zexiam C., Sung C., and Xiushau Z. (1985) Chemical dynamics of the Changjiang estuary. *Cont. Shelf Res.* **4,** 17–36.

Emerson D. and Moyer C. (1997) Isolation and characterization of novel iron-oxidizing bacteria that grow at circumneutral pH. *Appl. Environ. Microbiol.* **63,** 4784–4792.

Ford R. G., Bertsch P. M., and Farley K. J. (1997) Changes in transition and heavy metal partitioning during hydrous iron (hydr)oxide aging. *Environ. Sci. Technol.* **31,** 2028–2033.

Fredrickson J. K., Zachara J. M., Kennedy D. W., Duff M. C., Gorby Y. A., Li S.-M., and Krupa K. M. (2000) Reduction of U (VI) in goethite (a-FeOOH) suspension by a dissimilatory metal-reducing bacterium. *Geochim. Cosmochim. Acta* **64,** 3085–3098.

Froelich P. N., Klinkhammer G., Bender M. L., Luedtke N. A., Heath G. R., Cullen D., Dauphine P., Hammond D., Hartman B., and Maynard V. (1979) Early oxidation of organic matter in pelagic sediments of the eastern equatorial Atlantic: Suboxic diagenesis. *Geochim. Cosmochim. Acta* **43,** 1075–1090.

George G. N. (1993) EXAFSPAK. Stanford Synchrotron Radiation Laboratory.

Griffieon J. (1994) Uptake of phosphate by iron hydroxides during seepage in relation to development of groundwater composition in coastal areas. *Environ. Sci. Technol.* **28,** 675–681.

Hall G. E. M., Vaive J. E., Beer R., and Hoashi M. (1996) Selective leaches revisited, with emphasis on the amorphous Fe oxyhydroxide phase extraction. *J. Geochem. Explor.* **56,** 59–78.

Hansel C. M., Benner S. G., Neiss J., Dohnalkova A., Kukkadapu R. K., and Fendorf S. (2003) Secondary mineralization pathways induced by dissimilatory iron reduction of ferrihydrite under advective flow. *Geochim. Cosmochim. Acta* **67,** 2977–2992.

Hsi C.-K. D. and Langmuir D. (1985) Adsorption of uranyl onto ferric oxyhydroxides: Application of the surface complexation site-binding model. *Geochim. Cosmochim. Acta* **49,** 1931–1941.

Huettel M. and Gust G. (1992) Impact of bioroughness on interfacial solute exchange in permeable sediments. *Mar. Ecol. Prog. Ser.* **89,** 253–267.

Huettel M., Ziebis W., and Forster S. (1996) Flow-induced uptake of particulate matter in permeable sediments. *Limnol. Oceanogr.* **41,** 309–322.

Huettel M., Ziebis W., Forster S., and Luther G. W. III (1998) Advective transport affecting metal and nutrient distributions and interfacial fluxes in permeable sediments. *Geochim. Cosmochim. Acta* **62,** 613–631.

Huettel M. and Rusch A. (2000) Transport and degradation of phytoplankton in permeable sediment. *Limnol. Oceanogr.* **45,** 534–549.

Hunter K. A., Hawke D. J., and Choo L. K. (1988) Equilibrium adsorption of thorium by metal oxides in marine electrolytes. *Geochim. Cosmochim. Acta* **52,** 627–636.

Jahnke R. A., Alexander C. R., and Kostka J. E. (2003) Advective pore water input of nutrients to the Satilla River Estuary, Georgia, USA. *Estuar Coast. Shelf Sci.* **57,** 641–653.

Ingri J. and Ponter C. (1986) Iron and manganese layering in recent sediments in the Gulf of Bothnia. *Chem. Geol.* **56,** 105–116.

Klinkhammer G. P. and Palmer M. R. (1991) Uranium in the oceans: Where it goes and why. *Geochim. Cosmochim. Acta* **55,** 1799–1806.

Kristensen E., Kristensen K. D., and Jensen M. H. (2002) The influence of water column hypoxia on the behavior of manganese and iron in sandy coastal marine sediment. *Estuar. Coast. Shelf Sci.* **55,** 645–654.

Kristensen E., Kristensen K. D., and Jensen M. H. (2003) Temporal behavior of manganese and iron in a sandy coastal sediment exposed to water column anoxia. *Estuaries* **26,** 690–699.

Larson O. and Postma D. (2001) Kinetics of reductive bulk dissolution of lepidocrocite, ferrihydrite and goethite. *Geochim. Cosmochim. Acta* **65,** 1367–1379.

Lewis B. L. and Landing W. M. (1991) The biogeochemistry of manganese and iron in the Black Sea. *Deep-Sea Res.* **38** (Suppl.), S773–S803.

Li Y.-H. and Chan L. (1979) Desorption of Ba and ^{226}Ra from river-borne sediments in the Hudson estuary. *Earth Planet. Sci. Lett.* **43,** 343–350.

Li L., Barry D. A., Stangnitti F., and Parlange J.-Y. (1999) Submarine groundwater discharge and associated chemical input to a coastal sea. *Water Resour. Res.* **35,** 3253–3259.

Liger E., Charlet L., and van Cappellen P. (1999) Surface catalysis of uranium (VI) reduction by iron (II). *Geochim. Cosmochim. Acta* **63,** 2939–2955.

Lovely D. R. (1991) Dissimilatory Fe(III) and Mn(IV) reduction. *Microbiol. Rev.* **55,** 259–287.

Lovely D. R. and Phillips E. J. P. (1986) Organic matter mineralization with reduction of ferric iron in anaerobic sediments. *Appl. Environ. Microbiol.* **51,** 683–689.

Lovely D. R., Phillips E. P. Gorby Y. A., and Landa E. R. (1991) Microbial reduction of uranium. *Nature* **350,** 413–416.

Mayer T. D. and Jarrell W. M. (1996) Formation and stability of iron (III) oxidation products under natural concentrations of dissolved silica. *Water Res.* **30,** 1208–1214.

McKee B. A. and Todd J. F. (1993) Uranium behavior in a permanently anoxic fjord: Microbial control? *Limnol. Oceanogr.* **38,** 408–410.

Michael H. A., Lubetsky J. S., and Harvey C. F. (2003) Characterizing submarine groundwater discharge: A seepage meter study in Waquoit Bay, Massachusetts. *Geophys. Res. Lett.* **10.1029**/2002GL016000.

Mishra S. P. and Tiwary D. (1993) Radiotracer technique in adsorption studies. X. Efficient removal of Ba(II) from aqueous solutions by hydrous manganese oxide. *J. Radioanal. Nuclear Chem.* **170,** 133–141.

Mo T., Suttle A. D. and Sackett W. M. (1973) Uranium concentrations in marine sediments. *Geochim. Cosmochim. Acta* **37,** 35–51.

Montlucon D. and Sanudo-Wilhemey S. A. (2001) Influence of net groundwater discharge on the chemical composition of a coastal environment: Flanders Bay, Long Island, New York. *Environ. Sci. Technol.* **35,** 480–486.

Moore W. S. (1996) Large groundwater inputs to coastal waters revealed by ^{226}Ra enrichments. *Nature* **380,** 612–614.

Moore W. S. (1999) The subterranean estuary: A reaction zone of ground water and sea water. *Mar. Chem.* **65,** 111–125.

Moore W. S. and Shaw T. J. (1998) Chemical signals from fluid advection onto the continental shelf. *J. Geophy. Res.* **103,** 21543–21552.

Oldale R. N. (1976) Notes on the generalized geologic map of Cape Cod. U.S. Geological Survey Open-File Report 76-765.

Oldale R. N. (1981) *Pleistocene Stratigraphy of Nantucket, Martha's Vinyard, the Elizabeth Islands and Cape Cod, Massachusetts, Late Wisconsinan Glaciation of New England*. Dubuque, Iowa: Kendall/Hunt.

Parfitt R. L. (1989) Phosphate reactions with natural allophane, ferrihydrite and goethite. *J. Soil Sci.* **40,** 359–369.

Precht E. and Huettel M. (2003) Advective pore-water exchange driven by surface gravity waves and its ecological implications. *Limnol. Oceanogr.* **48,** 1674–1684.

Reimers C. E. Stecher H. A., Taghon G. L., Fuller C. M., Huettel M., Rusch A., Ryckelynck N., and Wild C. (2004) In situ measurements of advective solute transport in permeable shelf sands. *Cont. Shelf Res.* **24,** 183–201.

Roy H., Huettel M., and Jorgensen B. B. (2002) The role of small-scale sediment topography for oxygen flux across the diffusive boundary layer. *Limnol. Oceanogr.* **47,** 837–847.

Rusch A. and Huettel M. (2000) Advective particle transport into permeable sediments—Evidence from experiments in the intertidal sandflats. *Limnol. Oceanogr.* **45,** 525–533.

Shaw T. J., Sholkovitz E. R., and Klinkhammer G. (1994) Redox dynamics in the Chesapeake Bay: The effect on sediment/water uranium exchange. *Geochim. Cosmochim. Acta* **58,** 2985–2995.

Shaw T. J., Moore W. S., Kloepfer J., and Sochaski M. (1998) The flux of barium to the coastal waters of the southeastern USA: The importance of submarine groundwater discharge. *Geochim. Cosmochim. Acta* **62,** 3047–3054.

Sholkovitz E., Herbold C., and Charette M. (2003) An automated dye-dilution based seepage meter for the time-series measurement of submarine groundwater discharge. *Limnol. Oceanogr. Methods* **1,** 16–28.

Sima O. and Arnold D. (2002) Transfer of the efficiency calibration of germanium gamma-ray detectors using the GESPECOR software. *Appl. Rad. Isotop.* **56,** 71–75.

Slomp C. P., Vandergaast S. J., and Van Raaphorst W. (1996) Phosphorus binding by poorly crystalline iron (hydr)oxides in North Sea sediments. *Mar. Chem.* **52,** 55–73.

Slomp C. P., Malschaert J. F. P., Lohse L., and Van Raaphorst W. (1997) Iron and manganese cycling in different sedimentary environments on the North Sea continental margin. *Continental Shelf Res.* **17,** 1083–1117.

Stookey L. L. (1970) Ferrozine—A new spectrometric reagent for iron. *Anal. Chem.* **42,** 779–781.

Stumm W. and Morgan J. J. (1981) *Aquatic Chemistry.* Wiley.

Sugiyama M., Hori T., Kihara S., and Matsui M. (1992) A geochemical study of the specific distribution of barium in Lake Biwa, Japan. *Geochim. Cosmochim. Acta* **56,** 597–605.

Talbot J. M., Kroeger K. D., Rago A., Allen M. C., and Charette M. A. (2003) Nitrogen flux and speciation through the subterranean estuary of Waquoit Bay, Massachusetts. *Biol. Bull.* **205,** 244–245.

Testa J. M., Charette M . A., Sholkovitz E. R., Allen M. C., Rago A., and Herbold C. W. (2002) Dissolved iron cycling in the subterra-

nean estuary of a coastal bay: Waquoit Bay, Massachusetts. *Biol. Bull.* **203,** 255–256.

Thamdrup B., Fossing H., and Jorgensen B. B. (1994) Manganese, iron and sulfur cycling in a coastal marine sediment, Aarhus Bay, Denmark. *Geochim. Cosmochim. Acta* **58,** 5115–5129.

Torrent J., Schwertmann U., and Barron V. (1992) Fast and slow phosphate sorption by goethite-rich natural minerals. *Clays Clay Minerals* **40,** 14–21.

Ullman W. J., Chang B., Miller D. C., and Madsen J. A. (2003) Groundwater mixing, nutrient diagenesis and discharges across a sandy beachface, Cape Henlopen, Delaware (USA). *Estuar. Coast. Shelf Sci.* **57,** 539–552.

USGS [U.S. Geological Survey] (2003) *Ground Water in Freshwater-Saltwater Environments of the Atlantic Coast*. Circular 1262. U.S. Geological Survey.

Valiela I., Costa J., Foreman K., Teal J. M., Howes B., and Aubrey D. (1990) Transport of groundwater-borne nutrients from watersheds and their effects on coastal waters. *Biogeochemistry* **10,** 177–197.

Veeh H. H. (1967) Deposition of uranium from the oceans. *Earth Planet. Sci. Lett.* **3,** 145–150.

Windom H. and Niencheski F. (2003) Biogeochemical processes in a freshwater-seawater mixing zone in permeable sediments along the coast of Southern Brazil. *Mar. Chem.* **83,** 121–130.

Zachara J. M., Fredrickson J. K., Smith S. C., and Gassman P. L. (2001) Solubilization of Fe(III) oxide–bound trace metals by a dissimilatory Fe(III) reducing bacteria. *Geochim. Cosmochim. Acta* **65,** 75–93.

APPENDIX

Electronic Annex

Supplementary data associated with this article can be found, in the online version at doi:10.1016/j.gca.2004.10.024.